Addition and Metathesis Reactions of Zirconium and Hafnium Imido Complexes

Joseph L. Thorman,[†] Ilia A. Guzei,[†] Victor G. Young, Jr.,[‡] and L. Keith Woo*[,†]

Departments of Chemistry, Iowa State University, Ames, Iowa 50011-3111, and University of Minnesota, Minneapolis, Minnesota 55455

Received August 18, 1999

The zirconium and hafnium imido metalloporphyrin complexes (TTP)M═NAr$^{i\mathrm{Pr}}$ (TTP = *meso*-5,10,15,20-tetra-*p*-tolylporphyrinato dianion; M = Zr (**1**), Hf; Ar$^{i\mathrm{Pr}}$ = 2,6-diisopropylphenyl) were used to mediate addition reactions of carbonyl species and metathesis of nitroso compounds. The imido complexes react in a stepwise manner in the presence of 2 equiv of pinacolone to form the enediolate products (TTP)M[OC(*t*Bu)CHC(*t*Bu)(Me)O] (M = Zr (**2**), Hf (**3**)), with elimination of $H_2NAr^{i\mathrm{Pr}}$. The bis(μ-oxo) complex [(TTP)ZrO]$_2$ (**4**) is formed upon reaction of (TTP)Zr═NAr$^{i\mathrm{Pr}}$ with PhNO. Treatment of compound **4** with water or treatment of compound **2** with acetone produced the (μ-oxo)bis(μ-hydroxo)-bridged dimer [(TTP)Zr]$_2$(μ-O)(μ-OH)$_2$ (**5**). Compounds **2**, **4**, and **5** were structurally characterized by single-crystal X-ray diffraction.

Introduction

The preparation of group 4 chalcogenido complexes is an attractive goal in light of the high reactivity of metallocene and tetraazaannulene analogues described in a number of reports.[1−3] Notable examples include C−H bond activation, cycloaddition, and enolate formation. Toward this end, we have developed nitrene group and chalcogenido atom transfer routes with titanium metalloporphyrin complexes. Efforts to extend this methodology to the heavier congeners has now become an area of attention. In an ongoing investigation of group 4 metalloporphyrin imido complexes, we have found a number of novel reactivity properties.[4−6] We demonstrated previously that the imido complexes (TTP)M═NAr$^{i\mathrm{Pr}}$ (M = Zr, Hf) exhibit reactivity with heterocumulenes to form [2 + 2] cycloaddition products.[7] Further reactivity has been explored with other unsaturated substrates. Among these are pinacolone and PhNO, for which we now describe results found for their reactions with zirconium and hafnium imido complexes.

Experimental Section

General Procedures. All manipulations were performed under a nitrogen atmosphere using a Vacuum Atmospheres glovebox equipped with a model MO40-1 Dri-Train gas purifier. Benzene, benzene-d_6, toluene, THF, and hexane were freshly distilled from purple solutions of sodium benzophenone and brought into the drybox without exposure to air. The dichloro, (TTP)MCl$_2$, imido, (TTP)M═NAr$^{i\mathrm{Pr}}$ (M = Zr, Hf), and (TTP)Zr(η^2-NAr$^{i\mathrm{Pr}}$C(═N*t*Bu)O) compounds were prepared according to literature procedures.[7] Pinacolone was purchased from Aldrich, vacuum-transferred, and dried by passage through a plug of activated neutral alumina. Pinacolone-d_{12} was prepared according to a literature procedure.[8] ^{1}H and ^{13}C NMR data were acquired on Varian VXR (300 MHz, 20 °C) and Bruker DRX (400 MHz, 25 °C) spectrometers. Chemical shifts (ppm) are referenced to proton solvent impurities (δ 7.15, C_6D_5H). UV−vis data were recorded on a HP8452A diode array spectrophotometer and are reported as λ_{max} in nm (log ϵ). Elemental analyses (C, H, N) were performed by Iowa State University Instrument Services. GCMS studies were performed on a Varian gas chromatograph coupled to an ITS 40 ion trap mass spectrometer (capillary column DB-5MS).

(TTP)Zr(NHAr$^{i\mathrm{Pr}}$)[OC(*t*Bu)(═CH$_2$)], 2a. This complex was formed within minutes by treatment of the imido complex, **1**, with 1 equiv of pinacolone in toluene or benzene. Although complex **2a** is stable in its mother liquor for days at ambient temperature and at 80 °C, it could not be isolated in an analytically pure form. ^{1}H NMR (C_6D_6, 400 MHz): 9.18 (s, 8H, β-H), 8.55 (d, 4H, $^3J_{H-H}$ = 7 Hz, *meso*-$C_6H_4CH_3$), 7.85 (d, 4H, $^3J_{H-H}$ = 7 Hz, *meso*-$C_6H_4CH_3$), 7.33 (d, 4H, $^3J_{H-H}$ = 8 Hz, *meso*-$C_6H_4CH_3$), 7.23 (d, 4H, $^3J_{H-H}$ = 8 Hz, *meso*-$C_6H_4CH_3$), 6.22 (m, 3H, *m*,*p*-NHAr$^{i\mathrm{Pr}}$), 3.02 (s, 1H, OC(═C*H*$_2$)*t*Bu), 2.40 (s, 12H, *meso*-$C_6H_4CH_3$), 1.35 (s, 1H, OC(═C*H*$_2$)*t*Bu), 0.96 (s, 1H, N*H*Ar$^{i\mathrm{Pr}}$), 0.46 (d, 6H, $^3J_{H-H}$ = 8.9 Hz, 2,6-(CH(C*H*$_3$)$_2$)$_2$C$_6$H$_4$), 0.32 (d, 6H, $^3J_{H-H}$ = 8.6 Hz, 2,6-(CH(C*H*$_3$)$_2$)$_2$C$_6$H$_4$), −0.22 (m, 2H, 2,6-(C*H*(CH$_3$)$_2$)$_2$C$_6$H$_4$), −0.50 (s, 9H, OC(═CH$_2$)*t*Bu). ^{13}C NMR (C_6D_6): 170.7 (O*C*(═CH$_2$)*t*-Bu), 150.6, 148.6, 139.8, 137.1, 135.2 (*o*-tolyl), 134.2 (*o*-tolyl), 132.5 (β-pyrrole), 128.5 (*m*-tolyl), 125.6, 125.4, 121.2 (*m*,*p*-Ar$^{i\mathrm{Pr}}$), 119.7 (*m*,*p*-Ar$^{i\mathrm{Pr}}$), 83.3 (OC(═*C*H2)*t*Bu), 34.1, 29.0 (*C*H(Me)$_2$), 27.3 (OC(═CH$_2$)-(C(*C*H$_3$)$_3$), 24.6 (CH(*Me*)$_2$), 22.0 (CH(*Me*)$_2$), 21.4 (*C*H$_3$-tolyl).

(TTP)Zr[OC(*t*Bu)CHC(*t*Bu)(Me)O], 2. A solution of (TTP)Zr═NAr$^{i\mathrm{Pr}}$ (237 mg, 0.253 mmol) and pinacolone (200 μL, 1.60 mmol) in benzene (ca. 15 mL) was stirred at 25 °C for 40 h. This dark blue solution was filtered, and the filtrate was evaporated to dryness in vacuo to yield blue **2** (204 mg, 84% yield). UV/vis (toluene): 548 (4.55), 425 (5.66), 405 (shoulder, 3.23). ^{1}H NMR (C_6D_6, 300 MHz): 9.21 (m, 8H, β-H), 8.47 (d, 4H, $^3J_{H-H}$ = 7 Hz, *meso*-$C_6H_4CH_3$), 7.93 (d, 4H, $^3J_{H-H}$ = 7 Hz, *meso*-$C_6H_4CH_3$), 7.36 (d, 4H, $^3J_{H-H}$ = 8 Hz, *meso*-$C_6H_4CH_3$), 7.25 (d, 4H, $^3J_{H-H}$ = 8 Hz, *meso*-$C_6H_4CH_3$), 3.00 (s, 1H, OC(*t*Bu)C*H*C(*t*Bu)(Me)O), 2.40 (s, 12H, *meso*-$C_6H_4CH_3$), 0.04 (s, 9H, OC(*t*Bu)CHC(*t*Bu)(Me)O), −0.46 (s, 9H, OC(*t*Bu)CHC(*t*Bu)(Me)O),

[†] Iowa State University.
[‡] University of Minnesota.

(1) Carney, M. J.; Walsh, P. J.; Hollander, F. J.; Bergman, R. G. *Organometallics* **1992**, *11*, 761 and references therein.
(2) Howard, W. A.; Trnka, T. M.; Waters, M.; Parkin, G. *J. Organomet. Chem.* **1997**, *528*, 95 and references therein.
(3) Housmekerides, C. E.; Ramage, D. L.; Kretz, C. M.; Shontz, J. T.; Pilato, R. S.; Geoffroy, G. L.; Rheingold, A. L.; Haggerty, B. S. *Inorg. Chem.* **1992**, *31*, 4453.
(4) Berreau, L. M.; Young, V. G., Jr.; Woo, L. K. *Inorg. Chem.* **1995**, *34*, 527.
(5) Gray, S. D.; Thorman, J. L.; Berreau, L. M.; Woo, L. K. *Inorg. Chem.* **1997**, *36*, 278.
(6) Gray, S. D.; Thorman, J. L.; Adamian, V.; Kadish, K. M.; Woo, L. K. *Inorg. Chem.* **1998**, *37*, 1.
(7) Thorman, J. L.; Guzei, I. A.; Young, V. G., Jr.; Woo, L. K. *Inorg. Chem.* **1999**, *38*, 3814.
(8) Gilman, H. *Organic Syntheses*; John Wiley & Sons: New York, 1932; Collect. Vol. I, pp 48−452.

10.1021/ic9910007 CCC: $19.00
Published on Web 05/04/2000

−0.69 (s, 3H, OC(ᵗBu)CHC(ᵗBu)(*Me*)O); ^{13}C NMR (C_6D_6): 159.5 (OC(=CH)(ᵗBu)), 150.4 (α-pyrrole), 150.1 (α-pyrrole), 140.0, 137.4, 135.2 (*o*-tolyl), 134.5 (*o*-tolyl), 132.61 (*β*-pyrrole), 132.56 (*β*-pyrrole), 127.9 (*m*-tolyl, obscured by solvent), 127.8 (*m*-tolyl, obscured by solvent), 124.7, 97.6 (OC(=CH)(ᵗBu)), 80.0 (O*C*(Me)(ᵗBu)), 37.2, 34.8, 27.4 (OC(=CH)C*Me*$_3$), 24.3 (OC(Me)C*Me*$_3$), 23.7 (OC(*Me*)(ᵗBu)), 21.4 (*C*H$_3$-tolyl). Anal. Calcd (found) for $C_{60}H_{58}N_4O_2Zr$: C, 75.20 (75.35); H, 6.10 (6.19); N, 5.85 (5.59).

(TTP)Hf(NHAr^{iPr})[OC(ᵗBu)(=CH$_2$)], 3a. The formation of complex **3a** was observed in an NMR tube experiment. An NMR tube equipped with a Teflon stopcock was charged with (TTP)Hf=NAr^{iPr} (11.7 mg, 11.5 *μ*mol), Ph$_3$CH (91.0 *μ*L, 0.1439 M in C_6D_6, 13.0 *μ*mol), pinacolone (6.7 *μ*L, 53.6 *μ*mol), and C_6D_6 (ca. 0.6 mL). Complex **3a** (11.5 *μ*mol, 100% NMR yield) was formed after 17 h at 25 °C. Complex **3** (11.4 *μ*mol, 99% NMR yield) was formed after heating this solution for 25 h at 85 °C. ^{1}H NMR (C_6D_6, 400 MHz): 9.20 (s, 8H, *β*-H), 8.55 (d, 4H, $^3J_{H-H}$ = 7 Hz, *meso*-C$_6$*H*$_4$CH$_3$), 7.85 (d, 4H, $^3J_{H-H}$ = 7 Hz, *meso*-C$_6$*H*$_4$CH$_3$), 7.33 (d, 4H, $^3J_{H-H}$ = 8 Hz, *meso*-C$_6$*H*$_4$CH$_3$), 7.23 (d, 4H, $^3J_{H-H}$ = 8 Hz, *meso*-C$_6$*H*$_4$CH$_3$), 6.22 (m, 3H, *m*,*p*-NHAr^{iPr}), 2.91 (s, 1H, OC(=C*H*$_2$)ᵗBu), 2.40 (s, 12H, *meso*-C$_6$H$_4$C*H*$_3$), 1.18 (s, 1H, OC(=C*H*$_2$)ᵗBu), 0.88 (s, N*H*Ar^{iPr}, obscured by pinacolone), 0.48 (d, 6H, $^3J_{H-H}$ = 6.9 Hz, 2,6-(CH(C*H*$_3$)$_2$)$_2$C$_6$H$_4$), 0.31 (d, 6H, $^3J_{H-H}$ = 6.7 Hz, 2,6-(CH(C*H*$_3$)$_2$)$_2$C$_6$H$_4$), −0.17 (m, 2H, 2,6-(C*H*(CH$_3$)$_2$)$_2$C$_6$H$_4$), −0.50 (s, 9H, OC(=CH$_2$)ᵗ*Bu*).

(TTP)Hf[OC(ᵗBu)CHC(ᵗBu)(Me)O], 3. A solution of (TTP)Hf=NAr^{iPr} (128 mg, 0.125 mmol) and pinacolone (90 *μ*L, 0.72 mmol) in toluene (ca. 10 mL) was stirred at 25 °C for 140 h. The reaction had not reached completion at this time, and the mixture was subsequently heated for 26 h at 80 °C. This dark blue solution was filtered, and the filtrate was evaporated to dryness in vacuo and recrystallized from a toluene solution layered with hexanes at −25 °C overnight to yield blue **3** (79 mg, 61% yield). UV/vis (toluene): 548, 425. ^{1}H NMR (C_6D_6, 300 MHz): 9.23 (m, 8H, *β*-H), 8.47 (d, 4H, $^3J_{H-H}$ = 7 Hz, *meso*-C$_6$*H*$_4$CH$_3$), 7.91 (d, 4H, $^3J_{H-H}$ = 7 Hz, *meso*-C$_6$*H*$_4$CH$_3$), 7.35 (d, 4H, $^3J_{H-H}$ = 8 Hz, *meso*-C$_6$*H*$_4$CH$_3$), 7.24 (d, 4H, $^3J_{H-H}$ = 8 Hz, *meso*-C$_6$*H*$_4$CH$_3$), 2.92 (s, 1H, OC(ᵗBu)C*H*C(ᵗBu)(Me)O), 2.40 (s, 12H, *meso*-C$_6$H$_4$C*H*$_3$), 0.04 (s, 9H, OC(ᵗ*Bu*)CHC(ᵗBu)(Me)O), −0.43 (s, 9H, OC(ᵗBu)CHC(ᵗ*Bu*)(Me)O), −0.72 (s, 3H, OC(ᵗBu)CHC(ᵗBu)(*Me*)O.

[(TTP)ZrO]$_2$, 4. A solution of (TTP)Zr=NAr^{iPr} (214 mg, 0.228 mmol) and PhNO (28.2 mg, 0.263 mmol) in toluene (ca. 15 mL) was stirred at 25 °C for 1.5 h. This dark blue solution was filtered, and the filtrate was evaporated to dryness in vacuo to yield blue **4** (99 mg, 56% yield). UV/vis (toluene): 548 (4.38), 511 (4.51), 473 (4.40), 420 (5.56), 364 (4.41). ^{1}H NMR ($CDCl_3$, 300 MHz): 8.44 (s, 8H, *β*-H), 7.58 (m, 8H, *meso*-C$_6$*H*$_4$CH$_3$), 7.40 (m, 8H, *meso*-C$_6$*H*$_4$CH$_3$), 2.71 (s, 12H, *meso*-C$_6$H$_4$C*H*$_3$). ^{13}C NMR ($CDCl_3$): 148.0, 139.3, 136.8, 135.7 (*meso*-*C*$_6$H$_4$CH$_3$), 132.9 (*meso*-*C*$_6$H$_4$CH$_3$), 130.6 (*β*-pyrrole), 127.0 (*meso*-*C*$_6$H$_4$CH$_3$), 122.5, 21.5 (*meso*-C$_6$H$_4$*C*H$_3$). GC/MS (Ar^{iPr}N=NPh), *m*/*z*, calcd (found): 266.39 (266). Anal. Calcd (found) for $C_{96}H_{72}N_8O_2Zr_2$: C, 74.29 (74.38); H, 4.68 (5.29); N, 7.22 (6.60).

[(TTP)Zr]$_2$(*μ*-O)(*μ*-OH)$_2$, 5. A solution of **2** (129 mg, 0.135 mmol) and acetone (150 *μ*L, 2.04 mmol) in toluene (ca. 10 mL) was refluxed for 36 h. This dark blue solution was filtered, and the solid was washed with toluene (3 × 2 mL) to yield blue **5** (92 mg, 43% yield). UV/vis (CH_2Cl_2): 541 (4.64), 416 (5.75). ^{1}H NMR ($CDCl_3$, 300 MHz): 8.41 (s, 16H, *β*-H), 7.62 (bd, *meso*-C$_6$*H*$_4$CH$_3$), 7.46 (bd, *meso*-C$_6$*H*$_4$CH$_3$), 7.41 (bd, *meso*-C$_6$*H*$_4$CH$_3$), 2.71 (s, 24H, *meso*-C$_6$H$_4$C*H*$_3$), −8.27 (s, 2H, *μ*-OH). ^{13}C NMR ($CDCl_3$): 148.1, 139.2, 136.8, 130.4 (*β*-pyrrole), 129.0 (*meso*-*C*$_6$H$_4$CH$_3$), 128.2, 127.0, 125.3, 21.5 (*meso*-C$_6$H$_4$*C*H$_3$). Anal. Calcd (found) for $C_{96}H_{74}N_8O_3Zr_2$: C, 73.44 (73.99); H, 4.75 (4.91); N, 7.14 (6.48).

Reaction of Complex 2a with *p*-Toluidine. Complex **2a** was generated in situ in an NMR tube equipped with a Teflon stopcock. Within minutes of adding approximately 6 equiv of H$_2$N-tolyl, all NHAr^{iPr} in **2a** had been replaced by NH-tolyl to form (TTP)Zr(NH-tolyl)(OC(ᵗBu)(=CH$_2$)), **2b**. ^{1}H NMR (C_6D_6, 300 MHz): 9.14 (s, 8H, *β*-H), 8.46 (d, 4H, *meso*-C$_6$*H*$_4$CH$_3$), 7.85 (d, 4H, *meso*-C$_6$*H*$_4$CH$_3$), 7.35 (d, 4H, *meso*-C$_6$*H*$_4$CH$_3$), 7.22 (d, 4H, *meso*-C$_6$*H*$_4$CH$_3$), 6.29 (d, *m*-tolyl, obscured by H$_2$N-tolyl), 4.20 (d, 2H, *o*-tolyl), 3.00 (s, 1H, OC(=C*H*$_2$)ᵗ-Bu), 2.39 (s, 12H, *meso*-C$_6$H$_4$C*H*$_3$), 1.87 (s, 6H, *p*-*Me*C$_6$H$_4$) (OC(=C*H*$_2$)ᵗBu and N*H*Ar^{iPr} signals were not observed, obscured by pinacolone and H$_2$NAr^{iPr}), −0.26 (s, 9H, OC(=CH$_2$)ᵗ*Bu*). Addition of 2 equiv of pinacolone led to the formation of complex **2** within 15 min.

Reaction of Complex 2a with 2-Octanone. An NMR tube equipped with a Teflon stopcock was charged with (TTP)Zr=NAr^{iPr} (15.6 mg, 16.7 *μ*mol), Ph$_3$CH (93.0 *μ*L, 0.1397 M in C_6D_6, 13.0 *μ*mol), pinacolone (2.3 *μ*L, 18.4 *μ*mol), and C_6D_6 (ca. 0.6 mL). Allowing the tube to stand at 20 °C for 16 h afforded **2a** in quantitative yield, at which time 2-octanone (7.0 *μ*L, 44.7 *μ*mol) was added. Allowing this reaction mixture to stand at 20 °C for 23 h afforded (TTP)Zr(OC(ᵗBu)CHC(hexyl)(Me)O) (15.0 *μ*mol, 90% NMR yield). Complex **2** was not observed at any time during this reaction. Treatment of the final reaction mixture with water produced the enone as one of the many decomposition products. ^{1}H NMR (C_6D_6, 300 MHz): 9.21 (s, 8H, *β*-H), 8.41 (d, 4H, $^3J_{H-H}$ = 7 Hz, *meso*-C$_6$*H*$_4$CH$_3$), 7.91 (d, 4H, $^3J_{H-H}$ = 7 Hz, *meso*-C$_6$*H*$_4$CH$_3$), 7.37 (d, 4H, $^3J_{H-H}$ = 8 Hz, *meso*-C$_6$*H*$_4$CH$_3$), 7.24 (d, 4H, $^3J_{H-H}$ = 8 Hz, *meso*-C$_6$*H*$_4$CH$_3$), 2.84 (s, 1H, OC(ᵗBu)C*H*C(hexyl)(Me)O), 2.40 (s, 12H, *meso*-C$_6$H$_4$C*H*$_3$), 1.2−0.6 (m, OC(ᵗBu)C*H*C(*hexyl*)(Me)O, obscured by H$_2$NAr^{iPr}, pinacolone, and 2-octanone), 0.05 (s, 9H, OC(ᵗ*Bu*)CHC(hexyl)(Me)O), −0.29 (m, 2H, OC(ᵗBu)CHC(C*H*$_2$(CH$_2$)$_4$CH$_3$)(Me)O), −0.72 (s, 3H, OC(ᵗBu)CHC(hexyl)(*Me*)O. GC/MS (2,2,5-trimethyl-4-undecen-3-one, $C_{14}H_{26}O$), *m*/*z*, calcd (found): [M$^+$] 210.36 (211).

Reaction of (TTP)Zr(*η*^{2}-NAr^{iPr}C(=N^{t}Bu)O) with Pinacolone. An NMR tube equipped with a Teflon stopcock was charged with (TTP)Zr(*η*^{2}-NAr^{iPr}C(=N^{t}Bu)O) (13.1 mg, 12.68 *μ*mol), Ph$_3$CH (91.5 *μ*L, 0.1455 M in C_6D_6, 13.3 *μ*mol), pinacolone (7.0 *μ*L, 56.0 *μ*mol), and C_6D_6 (ca. 0.6 mL). Allowing the tube to stand at 20 °C for 15 h afforded **2** (11.5 *μ*mol, 90% NMR yield) and Ar^{iPr}NHC(O)NHᵗBu (9.2 *μ*mol, 72% NMR yield). GC/MS ($C_{17}H_{28}N_2O$), *m*/*z*, calcd (found): [M$^-$] 276.42 (277). ^{1}H NMR (C_6D_6, 300 MHz): 7.16 (*m*,*p*-C$_6$H$_3$, obscured by H$_2$NAr^{iPr}), 7.08 (d, 2H, *m*-C$_6$H$_3$, obscured by H$_2$NAr^{iPr}), 4.02 (s, 1H, NH), 3.57 (m, 2H, −C*H*Me$_2$), 1.23 (d, 12H, −CH*Me*$_2$), 1.18 (s, 9H, NC*Me*$_3$).

Structure Determinations of (TTP)Zr[OC(ᵗBu)CHC(ᵗBu)(Me)O] (2), [(TTP)ZrO]$_2$ (4), and [(TTP)Zr]$_2$(*μ*-O)(*μ*-OH)$_2$ (5). Crystal data can be found in Table 1. Compound **5** was treated by attachment to a glass fiber and mounting on a Siemens SMART system for data collection at 173(2) K. An initial set of cell constants was calculated from reflections harvested from three sets of 20 frames. These initial sets of frames were oriented such that orthogonal wedges of reciprocal space were surveyed. This produced orientation matrices determined from 154 reflections for compound **5**. Final cell constants were calculated from a set of 4170 strong reflections from the actual data collection. Three major swaths of frames were collected with 0.30° steps in *ω*. The space group was determined on the basis of systematic absences and intensity statistics, and a successful direct-methods solution was calculated which provided most non-hydrogen atoms from the *E*-map. Several full-matrix least squares/difference Fourier cycles were performed which located the remainder of non-hydrogen atoms. These were refined with anisotropic displacement parameters. Atom O1 was located on the crystallographic 2-fold axis and appeared to be a hydroxo ligand based on a long metal−oxygen bond length. The proton attached to O1 was assumed to be in an sp^3 geometry and disordered over the two possible, partially occupied sites. The other two oxygens, bridging hydroxide (O3) and oxo (O2), were equally disordered over the crystallographic 2-fold axis and were refined with restrained metal−oxygen distances. All hydrogen atoms were placed in ideal positions and refined as riding atoms with relative isotropic displacement parameters. There were 1.5 solvent molecules of benzene per asymmetric unit. SHELXTL DELU and SAME restraints were employed here to keep reasonable C−C distances and approximate rigid-body anisotropic displacement parameters. There were 48 restraints used altogether. Three bad reflections were omitted from the final least-squares refinement. All calculations were performed using SGI INDY R4400-SC or Pentium computers using the SHELXTL V5.0 program suite.[9]

Crystals of **2** and **4** were treated in an analogous manner to that of **5**. Systematic absences in the diffraction data were uniquely consistent

(9) *SHELXTL-Plus V5.0*; Siemens Industrial Automation, Inc.: Madison, WI, 1997.

Table 1. Crystal Data and Structure Refinements

	(TTP)Zr(OC(^{t}Bu)CHC(^{t}Bu)(Me)O)	[(TTP)ZrO]$_2$	[(TTP)Zr]$_2$(μ-O)(μ-OH)$_2$
empirical formula	$C_{76.50}H_{84}N_4O_2Zr$	$C_{110}H_{88}N_8O_2Zr_2$	$C_{114}H_{92}N_8O_3Zr_2$
fw	1182.70	1736.32	1804.40
temp, K	173(2)	173(2)	173(2)
wavelength, Å	0.710 73	0.710 73	0.710 73
crystal system	monoclinic	monoclinic	monoclinic
space group	*Cc*	*C*2/*c*	*C*2/*c*
Unit cell dimens			
a, Å	21.8318(8)	31.8540(16)	32.0930(7)
b, Å	20.7139(8)	16.7937(8)	16.8621(3)
c, Å	15.7878(8)	18.8770(9)	19.0706(4)
β, deg	112.624(1)	117.254(1)	118.930(1)
V, Å^3	6590.2(5)	8977.1(8)	9032.3(3)
Z	4	4	4
density (calcd), Mg/m^3	1.192	1.285	1.327
abs coeff, mm^{-1}	0.215	0.289	0.291
F(000)	2508	3600	3744
crystal size, mm^3	0.30 × 0.30 × 0.30	0.21 × 0.40 × 0.42	0.35 × 0.26 × 0.13
θ range, deg	1.41−21.97	2.48−28.32	1.41−25.07
index ranges	$-22 \le h \le 22$	$-42 \le h \le 37$	$-38 \le h \le 33$
	$0 \le k \le 21$	$0 \le k \le 22$	$0 \le k \le 20$
	$-16 \le l \le 16$	$0 \le l \le 25$	$0 \le l \le 22$
no. of reflns collected	20 673	53 684	22 019
no. of indep reflns	7601 (R_{int} = 0.0337)	10 734 (R_{int} = 0.0687)	7894 (R_{int} = 0.0434)
abs cor	empirical with SADABS	SADABS	SADABS (Sheldrick, 1996)
max and min transm	0.9383 and 0.9383		1.000 and 0.716
refinement method	full-matrix least-squares on F^2	full-matrix least-squares on F^2	full-matrix least-squares on F^2
data/restraints/params	7601/233/544	10734/0/488	7891/48/583
goodness-of-fit on F^2	1.065	1.007	1.030
final *R* Indices [$I > 2\sigma(I)$][a]	R1 = 0.0691, wR2 = 0.1909	R1 = 0.0461, wR2 = 0.1068	R1 = 0.0553, wR2 = 0.1348
R indices (all data)[a]	R1 = 0.0828, wR2 = 0.2084	R1 = 0.0848, wR2 = 0.1133	R1 = 0.0840, wR2 = 0.1526
largest diff peak and hole, e Å^{-3}	1.292 and −0.690	0.587 and −0.435	0.855 and −0.828

[a] $R1 = \sum||F_o| - |F_c||/\sum|F_o|$. $wR2 = [\sum w(F_o^2 - F_c^2)^2/\sum w(F_o^2)^2]^{0.5}$; $w = 1/[\sigma^2(F_o^2) + (XP)^2 + (YP)]$ where $P = (\max(F_o^2, 0) + 2F_c^2)/3$ and *X* and *Y* are adjusted for each refinement.

for space groups denoted in Table 1. The structures were solved using direct methods, completed by subsequent difference Fourier synthesis, and refined by full-matrix least-squares procedures. For complex **2**, all porphyrin non-hydrogen atoms and zirconium were refined with anisotropic displacement coefficients. All other non-hydrogen atoms were refined isotropically. The enediolate ligand exhibited high thermal activity and was refined with an idealized geometry. The crystal was refined as a twin with a 52:48 ratio contribution from the two components. There were three severely disordered solvent molecules also present in the asymmetric unit, which were identified and accounted for as a hexane, toluene, and a half toluene molecule using the SQUEEZE option in the PLATON[10] program. PLATON calculated the upper limit of volume that can be occupied by the solvent to be 2028.3 Å^3, or 30.8% of the unit volume. The program calculated 512 electrons, which corresponds to four hexane and six toluene molecules, in the unit cell for the diffuse species. A similar treatment was applied to two severely disordered toluene molecules that were identified and refined in the asymmetric unit of complex **4**. PLATON calculated the upper limit of volume that could be occupied by the solvent to be 2016.5 Å^3, or 22.5% of the unit volume. The program calculated 812 electrons, corresponding to eight toluene molecules, in the unit cell for the diffuse species. Note that all derived data in the following tables were based on known contents. No data are given for the diffusely scattering solvent molecules.

Results

Pinacolone Coupling Mediated by (TTP)Zr═NAr^{iPr}, 1. Upon treatment of (TTP)Zr═NAr^{iPr}, **1**, with 1 equiv of pinacolone, a new species was observed within 5 min. Product analysis was achieved by ^{1}H NMR spectroscopy.[11] The observation of a three-proton multiplet at 6.22 ppm, due to the meta and para Ar^{iPr} protons, indicated that the NAr^{iPr} moiety had been retained in the product. This chemical shift is close to the upfield signals found for the corresponding aryl protons of the imido complex, **1**, at 6.08 ppm. Additionally, the new Ar^{iPr} isopropyl proton chemical shifts, 0.46 (d, 6H), 0.32 (d, 6H), −0.23 (m, 2H) ppm, remain significantly upfield of those of the free amine [2.63 (spt, 2H), 1.14 (d, 12H) ppm] and only slightly downfield from those found for complex **1** [0.18 (m, 2H), 0.00 (d, 12H) ppm]. The NH amido proton was observed at 0.95 ppm, similar to the chemical shifts reported for (TTP)Hf(N*H*Ph)(N*H*Ar^{iPr}).[7] Signals at 3.02 (s, 1H), 1.35 (s, 1H), and −0.50 (s, 9H) ppm signify the presence of a single bound pinacolone fragment. The large variation in chemical shifts for the two geminal protons (vide infra) was unusual but must arise because of differences in position relative to the porphyrin ring current.

Three possible limiting isomers for this product, consistent with the ^{1}H NMR data, are shown in Figure 1. Distinctive ^{13}C NMR resonances attributed to the bound pinacolone fragment, but not due to the *tert*-butyl group, are found at 83.3 and 170.7 ppm. A HETCOR experiment revealed that the protons resonating at 3.02 and 1.35 ppm were both bound to the same carbon atom (83.3 ppm), precluding isomer **I**. The proton resonating at 3.02 ppm displayed a through-space interaction with the *tert*-butyl group (−0.50 ppm) in a NOESY experiment. Consequently, this proton must be cis to the *tert*-butyl group. The ^{13}C NMR data are incompatible with isomer **II** because the peak

(10) All software and sources of the scattering factors are contained in the SHELXTL V5.10 program library: G. Sheldrick, Siemens-AXS, Madison, WI.

(11) The large ring current of the aromatic porphyrin macrocycle provides a useful means for identifying metal-bound ligands through ^{1}H NMR. Upfield shifts of bound-ligand protons are commonly 1−4 ppm from those of the free ligand. The ring current effects on the ^{13}C nuclei of metal-bound ligands of metalloporphyrin complexes are shifted to a smaller degree, which allows comparison of these resonances to those found in spectra of nonporphyrin metal analogues.

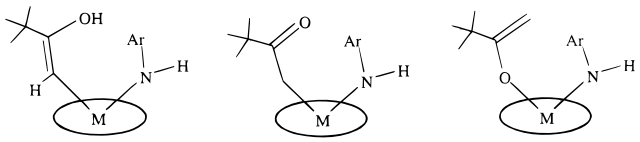

I **II** **III**

Figure 1. Possible isomers from the addition reaction between complex **1** and pinacolone.

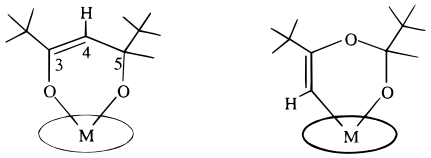

IV **V**

Figure 2. Possible isomers of coupled-pinacolone derivatives consistent with ^{1}H NMR data.

at 83.3 ppm is too far downfield for a C-bound enolate.[12] A metallocene enolate complex, Cp*$_2$Zr(OH)[η^1-OC(=CH$_2$)(^{t}Bu)], possesses similar ^{13}C NMR chemical shifts at 84.1 [OC(^{t}Bu)=*C*H$_2$] and 172.8 ppm [O*C*(=CH$_2$)(^{t}Bu)].[2] The NMR data for the addition product are most consistent with an O-bound enolate, isomer **III**. The enolato complex (TTP)Zr(NHAr$^{i\mathrm{Pr}}$)-[OC(=CH$_2$)(^{t}Bu)], **2a**, could not be isolated in pure form because of decomposition to intractable products during purification attempts.

Treatment of complex **2a** with 1 equivalent of pinacolone resulted in the elimination of H$_2$NAr$^{i\mathrm{Pr}}$ and formation of a metalloporphyrin product, **2**, containing two pinacolone fragments. The ^{1}H NMR integrations of the double-condensation product were consistent with the overall loss of two hydrogens from the two pinacolone molecules. A singlet at 3.00 ppm was assigned to an olefinic proton that had been shifted upfield by the porphyrin ring current. Two ^{t}Bu groups were observed as singlets at 0.04 (9H) and −0.46 (9H) ppm, and a methyl singlet appeared at −0.69 (3H) ppm. When a toluene-d_8 solution of complex **2** was cooled, broadening of the *tert*-butyl singlet at −0.46 ppm was observed in the ^{1}H NMR. At 234 K, this singlet had nearly broadened into the baseline while the geminal methyl signal (−0.69 ppm) remained sharp.[13] An unusual feature of complex **2** is the β-pyrrole proton resonance. This signal appears as an AB quartet (9.21 ppm, $^3J_{\mathrm{H-H}} = 4.6$ Hz, $\delta\nu = 4.8$ Hz) due to a stereogenic center in the product ligand. Two isomers that are consistent with the 1-D ^{1}H NMR data for the two coupled pinacolone molecules are shown in Figure 2.

The position of the olefinic proton was established by a NOESY experiment which showed through-space interactions of this hydrogen with both *tert*-butyl groups and the methyl group. Furthermore, the methyl group, which resonates at −0.69 ppm, was also close, spatially, to the *tert*-butyl unit with the signal at −0.46 ppm. Isomer **IV** was consistent with the NOESY experiment, while isomer **V** would exhibit an NOE interaction of the olefinic proton with only one ^{t}Bu group. The connectivity of the hydrocarbon backbone was definitively established by a HMBC experiment that showed two-bond coupling interactions between the olefinic proton and both carbon 3 and carbon 5 (see Figure 2 for numbering). Isomer **V** would contain a two-bond coupling of the olefinic proton to only one carbon atom. The chemical shifts of carbon 3 (160.0 ppm), carbon 4 (97.6 ppm), and carbon 5 (80.0 ppm) of the metallacycle backbone were assigned by HETCOR and HMBC NMR experiments.

In addition to 2-D NMR results, support for the assignment of the two *tert*-butyl groups in complex **2** was facilitated by deuterium labeling. Treatment of the imido complex **1** with 1 equiv of pinacolone followed by excess pinacolone-d_{12} produced complex **2** with a 9-proton singlet in the ^{1}H NMR spectrum at 0.04 ppm. Conversely, treatment of complex **1** with 1 equiv of pinacolone-d_{12} and then with excess pinacolone-d_0 produced enediolate complex **2** with a 9-proton singlet at −0.46 ppm and a 3-proton singlet at −0.69 ppm. These experiments also revealed that the source of the protons transferred to the imido group was the methyl group of the first pinacolone consumed. On the basis of the NMR structural analysis, the reaction sequence for pinacolone condensation with complex **1** is shown in eqs 1 and 2.

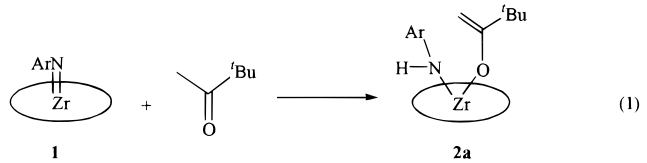

1 **2a** (1)

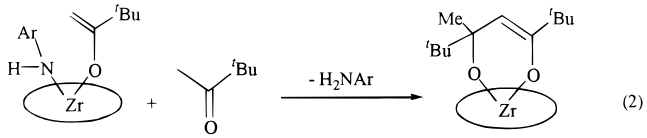

2a **2** (2)

Complex **2** could also be synthesized by alternate routes. Formation of the enediolate compound **2** occurred on treatment of the ureato complex (TTP)Zr(η^2-NAr$^{i\mathrm{Pr}}$C(=N^{t}Bu)O) with excess pinacolone. The urea, NHAr$^{i\mathrm{Pr}}$C(=O)NH^{t}Bu, was a byproduct of this process. Treatment of (TTP)ZrCl$_2$ with excess pinacolone in the presence of piperidine also resulted in the formation of complex **2**. Although this was a more direct synthetic approach, it yielded impure product. A one-pot synthesis that involved adding excess pinacolone to in situ generated complex **1** produced complex **2** in a yield and purity comparable to those found for the reaction with isolated imido complex **1**. Whereas the formation of complex **2** from enolate species **2a** required hours to reach completion, treatment of complex **2b** (the less bulky tolylamido analogue of **2a**) with pinacolone resulted in the rapid formation of the enediolate compound.

The preceding investigation also employed hafnium in place of zirconium. Due to similarities of the two series of compounds, only the latter was addressed. The largest difference in the ^{1}H NMR data of the amido/enolato congeners was found for the methylene resonances. The geminal CH$_2$ resonances for **3a** (2.91, 1.18 ppm) were slightly upfield of those for **2a** (3.02, 1.35 ppm). Similarly, the olefinic resonance in the enediolate complex was upfield for the hafnium derivative (2.92 ppm) relative to that for the zirconium complex (3.00 ppm). Reaction times were observed to be somewhat longer for the heavier congener, as observed previously for other Hf and Zr metalloporphyrin complexes.[7] Under identical reaction conditions, treatment of the respective imido complex, (TTP)M=NAr$^{i\mathrm{Pr}}$ (M = Zr, Hf), with excess pinacolone produced the amide/enolate complex within minutes for zirconium and 1 h for hafnium.

(12) (a) Stack, J. G.; Doney, J. J.; Bergman, R. G.; Heathcock, C. H. *Organometallics* **1990**, *9*, 453 and references therein. (b) Wanat, R. A.; Collum, D. B. *Organometallics* **1986**, *5*, 120.

(13) Conformational changes of the six-membered ring may serve as a possible source of disorder in the metallacycle as observed in the X-ray structure analysis.

Formation of Oxygen-Bridged Dimers 4 and 5. The bis(μ-oxo) complex [(TTP)ZrO]$_2$, **4**, was initially observed in the thermal decomposition of the N,O-bound ureato complexes (TTP)Zr[η^2-NAr$^{i\mathrm{Pr}}$C(=N^{t}Bu)O] and (TTP)Zr[η^2-N^{t}BuC(=NAr$^{i\mathrm{Pr}}$)-O].[7,14] A more facile route to complex **4** was found from the metathesis reaction between complex **1** and PhNO (eq 3). The

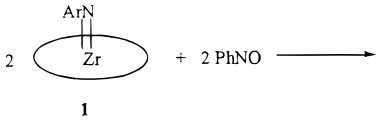

1

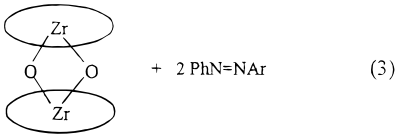

(3)

4

dimer was formed in moderate yield along with the diazene PhN=NAr$^{i\mathrm{Pr}}$. The ^{1}H NMR spectrum of the bis(μ-oxo) species exhibited signals typical of zirconium metalloporphyrin complexes. The exception was an upfield shift of the β-pyrrole signal to 8.44 ppm due to the face-to-face orientation of the two porphyrin rings. The β-pyrrole signal remained as a singlet at 223 K in $CDCl_3$, indicating fast rotation of the porphyrin rings relative to one another. Complex **4** readily undergoes hydrolysis upon exposure to water to produce the (μ-oxo)bis(μ-hydroxo) dimer, complex **5** (eq 4). The most facile preparation of

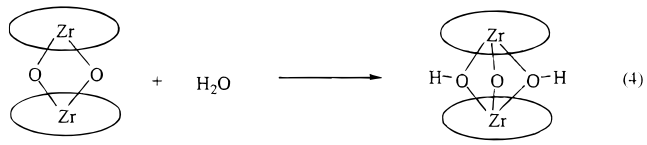

(4)

4 **5**

compound **5** was found from heating a toluene solution of complex **2** in the presence of excess acetone. The hydroxyl protons at −8.27 ppm (s, 2H) were found to be upfield of those reported for the tetraphenylporphyrin analogue (−6.73 ppm, s, 2H).[15b]

Crystal Structures of (TTP)Zr(OC(^{t}Bu)CHC(^{t}Bu)(Me)O) (2), [(TTP)ZrO]$_2$ (4), and [(TTP)Zr]$_2$(μ-O)(μ-OH)$_2$ (5). The crystallographic data for complexes **2**, **4**, and **5** are presented in Table 1, and selected metrical parameters are collected in Tables 2 and 3. All of the molecules exhibit typical out-of-plane displacements of the zirconium from the mean 4-N$_{\mathrm{pyrrole}}$ plane for six- and seven-coordinate metals. In the case of complex **2**, acquisition of high-quality crystals was not possible, despite numerous recrystallizations. These difficulties were attributed to the solvent-dependent nature of the crystals and volatile solvent molecules packed in the voids of the lattice. While extensive disorder in the enediolate ligand precluded anisotropic refinement of the carbon backbone, the oxygen atom identities were unequivocally established and were consistent

Table 2. Selected Bond Distances (Å) For Complexes **2**, **4**, and **5**

2		**4**		**5**	
Zr−O1	1.963(6)	Zr1−O1	1.9719(16)	Zr1−O1	2.166(3)
Zr−O2	1.945(7)	Zr1−O2	1.9791(16)	Zr1−O2	1.988(4)
				Zr1−O3	2.171(5)
Zr−N1	2.254(8)	Zr1−N1	2.246(2)	Zr1−N1	2.291(3)
Zr−N2	2.290(10)	Zr1−N2	2.280(2)	Zr1−N2	2.279(3)
Zr−N3	2.177(9)	Zr1−N3	2.241(2)	Zr1−N3	2.266(3)
Zr−N4	2.295(9)	Zr1−N4	2.280(2)	Zr1−N4	2.286(3)
Zr−N$_4$[a]	0.98		0.97		1.04

[a] Zr displacement from N_4 plane.

with the results of spectroscopic experiments. A representation of complex **2** is given in Figure 3. The Zr−O bond distances of 1.963(6) [Zr−O1] and 1.945(7) Å [Zr−O2] compare well with those in alkoxido compounds[16] but are considerably shorter than the single bonds observed in the four-atom metallacycles (TTP)Zr(η^2-NAr$^{i\mathrm{Pr}}$C(=N^{t}Bu)O) [2.0677(12) Å] and (TTP)Zr-(η^2-N^{t}BuC(=NAr$^{i\mathrm{Pr}}$)O) [2.066(3) Å].[7] Atom O1 eclipses the Zr−N2 bond within 2.0°, while atom O2 is staggered in relation to the Zr−N3 and Zr−N4 bonds by 62.5 and 26.5°, respectively. The Zr−N2 [2.290(10) Å] and Zr−N4 [2.295(9) Å] bonds are long compared to Zr−N3 [2.177(9) Å] and Zr−N1 [2.254(8) Å] distances. These differences are likely due to contributions from nitrogen−oxygen repulsions [N2−O1 = 2.717(2) Å; N4−O2 = 2.721(2) Å].[17]

Compound **4** (Figure 4) results from the formal dimerization of two (TTP)Zr=O units. The metal−oxygen bond distances, 1.9719(16) and 1.9791(16) Å [Zr1−O1 and Zr1−O2], are elongated compared to those of known oxo-bridged analogues but still suggest the presence of multiple bonding.[18] The oxygen atoms in complex **4** are staggered with respect to the Zr−N$_{\mathrm{pyrrole}}$ bonds. The O2−Zr1−Zr1A−N4A torsion angle is 33.8° and that of O2−Zr1−Zr1A−N3A is 57.3°. The positions of the bridging oxygen atoms lying closer to the N2 and N4 atoms may explain the variation in the Zr−N$_{\mathrm{pyrrole}}$ bond distances

(14) (a) The bis(μ-oxo) complex was reported previously, but no details on characterization were provided: Sewchok, M. G.; Haushalter, R. C.; Merola, J. S. *Inorg. Chim. Acta* **1988**, *144*, 47. (b) The unisolated octaethylporphyrin analogue of complex **4** has been characterized by ^{1}H NMR: Brand, H.; Arnold, J. *Organometallics* **1993**, *12*, 3655.

(15) (a) Huhmann, J. L.; Corey, J. Y.; Rath, N. P.; Campana, C. F. *J. Organomet. Chem.* **1996**, *513*, 17. (b) Kim, H. J.; Whang, D.; Do, Y.; Kim, K. *Chem. Lett.* **1993**, 807. (c) Kim, H.; Whang, D.; Kim, K.; Do, Y. *Inorg. Chem.* **1993**, *32*, 360. (d) Ryu, S.; Whang, D.; Kim, J.; Yeo, W.; Kim, K. *J. Chem. Soc., Dalton Trans.* **1993**, 205. (e) Ryu, S.; Kim, J.; Yeo, H.; Kim, K. *Inorg. Chim. Acta* **1995**, *228*, 233.

(16) Pertinent complexes with Zr−O bonds (Zr−O bond distance (Å); Zr−O−Zr bond angle (deg)) are as follows. (a) Cp$_2$Zr(OC(Me)$_2$C(TMS)C-(TMS)] (1.936(2)): Rosenthal, U.; Ohff, A.; Baumann, W.; Tillack, A.; Gorls, H.; Burlakov, V. V.; Shur, V. B. *J. Organomet. Chem.* **1994**, *484*, 203. (b) Cp*$_2$Zr(OCH$_2$CH$_2$CH$_2$) (2.008(13)): Mashima, K.; Yamakawa, M.; Takaya, H. *J. Chem. Soc., Dalton Trans.* **1991**, 2851. (c) (Me$_4$taen)Zr(O^{t}Bu)$_2$ (1.947 average): Black, D. G.; Jordan, R. F.; Rogers, R. D. *Inorg. Chem.* **1997**, *36*, 103. (d) Cp$_2$Zr(OPh)$_2$ (2.008(14) average): Howard, W. A.; Trnka, T. M.; Parkin, G. *Inorg. Chem.* **1995**, *34*, 5900. (e) (OEP)Zr(O^{t}Bu)$_2$ (1.948 average): ref 14b. (f) Cp*$_2$Zr(OH)(OC(^{t}Bu)(CH$_2$)) (2.001(6) for OH, 2.006(5) for enolate): ref 2. (g) Cp*$_2$Zr(OH)(OC(Ph)(CH$_2$)) (2.010(2) for OH, 1.993-(2) for enolate): Howard, W. A.; Parkin, G. *J. Am. Chem. Soc.* **1994**, *116*, 606. (h) Cp′$_2$Zr(O)(py) (1.804(4)): Howard, W. A.; Waters, M.; Parkin, G. *J. Am. Chem. Soc.* **1993**, *115*, 4917. (i) [Cp$_2$ZrO]$_3$ (1.959-(3), 142.5(2)): Fachinetti, G.; Floriani, C.; Chiesi-Villa, A.; Guastini, C. *J. Am. Chem. Soc.* **1979**, *101*, 1767. (j) [Cp$_2$ZrMe]$_2$O (1.948(1), 174.1): Hunter, W. E.; Hrncir, D. C.; Vann Bynum, R.; Penttila, R. A.; Atwood, J. L. *Organometallics* **1983**, *2*, 750. (k) [Cp$_2$ZrCl]$_2$O (1.94(5), 168.9(8)): Clarke, J. F.; Drew, M. G. B. *Acta Crystallogr. B* **1974**, *30*, 2267. (l) [((TMS)$_2$N)$_2$ZrMe]$_2$O (1.950, 180.0): Planalp, R. P.; Andersen, R. A. *J. Am. Chem. Soc.* **1983**, *105*, 7774. (m) [Cp$_2$-Zr(C(TMS)CH(TMS))]$_2$O (1.973(1)): Rosenthal, U.; Ohff, A.; Michalik, M.; Gorls, H.; Burlakov, V. V.; Shur, V. B. *Organometallics* **1993**, *12*, 5016. (n) [Cp$_2$Zr(triflate)]$_2$O (1.946(1), 175.6(5)): Calderazzo, F.; Englert, U.; Pampaloni, G.; Tripepi, G. *J. Organomet. Chem.* **1998**, *555*, 49. (o) [Cp$_2$Zr(SPh)]$_2$O (1.968(3), 165.8(2)): Petersen, J. L. *J. Organomet. Chem.* **1979**, *166*, 179. (p) [Cp$_2$Zr(NCO)]$_2$O (1.946(3), 165.7(2)): Klouras, N.; Tzavellas, N.; Raptopoulou, C. P. *Z. Anorg. Allg. Chem.* **1997**, *623*, 1027.

(17) van der Waals radii: O (1.52 Å), N (1.55 Å); Porterfield, W. W. *Inorganic Chemistry*; 2nd ed.; Academic Press: San Deigo, CA, 1998; p 214.

(18) Covalent radii estimates (Å): (a) O = 0.66; Jolly, W. L. *Modern Inorganic Chemistry*; McGraw-Hill: New York, 1984; p 52. (b) Zr = 1.48, O = 0.73; ref 17.

Table 3. Selected Bond Angles (deg) for Complexes **2**, **4**, and **5**

2		**4**		**5**	
O1−Zr−O2	76.9(3)	O1−Zr1−O2	78.56(8)	O1−Zr1−O2	76.1(2)
				O1−Zr1−O3	66.6(2)
				O2−Zr1−O3	74.0(2)
		Zr−O−Zr	101.64(12) av	Zr−O1−Zr	89.91(14)
				Zr−O2−Zr	100.6(3)
				Zr−O3−Zr	89.7(2)
N1−Zr−N3	131.97(18)	N1−Zr1−N3	130.35(8)	N1−Zr1−N3	125.83(11)
N2−Zr−N4	124.85(19)	N2−Zr1−N4	127.86(7)	N2−Zr1−N4	125.60(11)

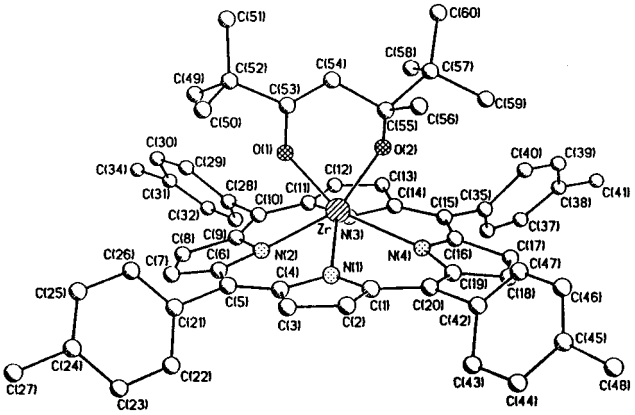

Figure 3. Ball and stick representation of complex **2**, (TTP)Zr[OC(ᵗBu)CHC(ᵗBu)(Me)O].

resulting from O−N interactions. The Zr1−Zr1A (3.0584(5) Å) and the O−O distances (2.5014 Å) are similar to those of previously described bridging zirconium porphyrin complexes.[15a,b] Three common distortions from planarity of the porphyrin macrocycle were observed in complex **4**.[19] The doming effect was readily perceived in the deviations of the four pyrrole nitrogens from the 24-atom porphyrin plane [11 (N1), 7 (N2), 17 (N3), and 9 (N4) pm]. The meso carbon atoms alternate above and below the mean 24-atom plane [15 (C5), −12 (C10), 16 (C15), and −12 (C20) pm] in a ruffling deformation. Although the saddle deformation of the porphyrin ring is perturbed by the presence of the other two distortions, it is observed in the deviations of the β-pyrrole atoms above and below the core porphyrin plane [−24 (C2), −15 (C3), 10 (C7), 1 (C8), −29 (C12), −19 (C13), 8 (C17), 2 (C18) pm].

The samples of $[(TTP)Zr]_2(\mu\text{-}O)(\mu\text{-}OH)_2$, **5**, produced in this work are closely related to the previously described tetraphenylporphyrin derivatives $[(TPP)Zr(\mu\text{-}OH)2]_2$[15a] and $[(TPP)Zr]_2(\mu\text{-}O)(\mu\text{-}OH)_2$.[15b] However, the OH proton resonance in complex **5** (−8.27 ppm) was significantly shifted from those of the tetrahydroxy- (−6.79 ppm) and the tetraphenylporphyrin dihydroxy analogues (−6.73 ppm). Consequently, compound **5** was examined in a single-crystal X-ray diffraction study. The zirconium coordination environment and metrical parameters are unremarkable from those previously described by Kim and co-workers for $[(TPP)Zr]_2(\mu\text{-}O)(\mu\text{-}OH)_2$. However, the presence of staggered porphyrin rings in complex **5** (Figure 5) is in marked contrast to the other structurally characterized oxygen-bridged Zr and Hf metalloporphyrin species.[15] The most acute torsion angle present in complex **5** involving a $Zr-N_{pyrrole}$ bond is 22.2° (N3−Zr1−Zr1A−N2A), whereas the corresponding angle in the TPP species is only 7.8°. The intramolecular

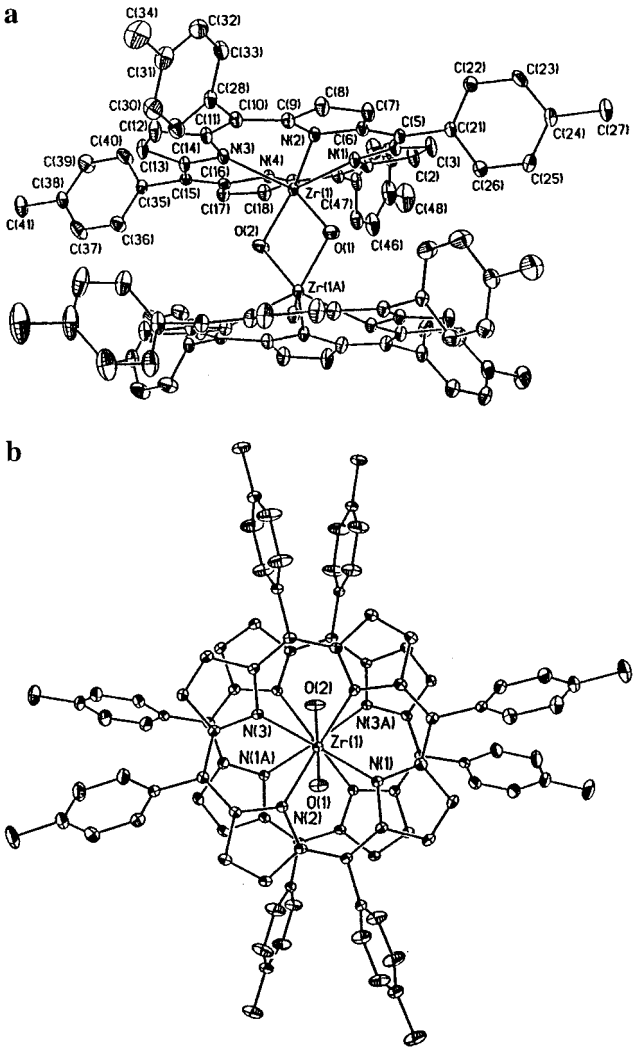

Figure 4. Molecular structure of $[(TTP)ZrO]_2$ (**4**). Thermal ellipsoids are drawn at the 30% probability level: (a) side view; (b) top view.

distance between the two 20-carbon atom mean planes of the porphyrins is equivalent for complexes **4** and **5** [5.3(2) Å].

Discussion

Coupling of Pinacolone by (TTP)M=NAr^{iPr} (M = Zr, Hf). The reactivity of the nitrene group in terminal zirconium and hafnium imido complexes has been documented in a number of studies.[7,20] A comparable example of a Zr=X moiety reacting with a ketone occurs with $Cp^*_2Zr(=O)(py)$ and acetophenone,

(19) Jentzen, W.; Simpson, M. C.; Hobbs, J. D.; Song, X.; Ema, T.; Nelson, N. Y.; Medforth, C. J.; Smith, K. M.; Veyrat, M.; Mazzanti, M.; Ramasseul, R.; Marchon, J.-C.; Takeuchi, T.; Goddard, W. A., III.; Shelnutt, J. A. *J. Am. Chem. Soc.* **1995**, *117*, 11085.

(20) (a) Walsh, P. J.; Hollander, F. J.; Bergman, R. G. *J. Am. Chem. Soc.* **1988**, *110*, 8729. (b) Cummins, C. C.; Baxter, S. M.; Wolczanski, P. T. *J. Am. Chem. Soc.* **1988**, *110*, 8731. (c) Walsh, P. J.; Hollander, F. J.; Bergman, R. G. *Organometallics* **1993**, *12*, 3705. (d) Blake, A. J.; Mountford, P.; Nikonov, G. I.; Swallow, D. *J. Chem. Soc., Chem. Commun.* **1996**, 1835.

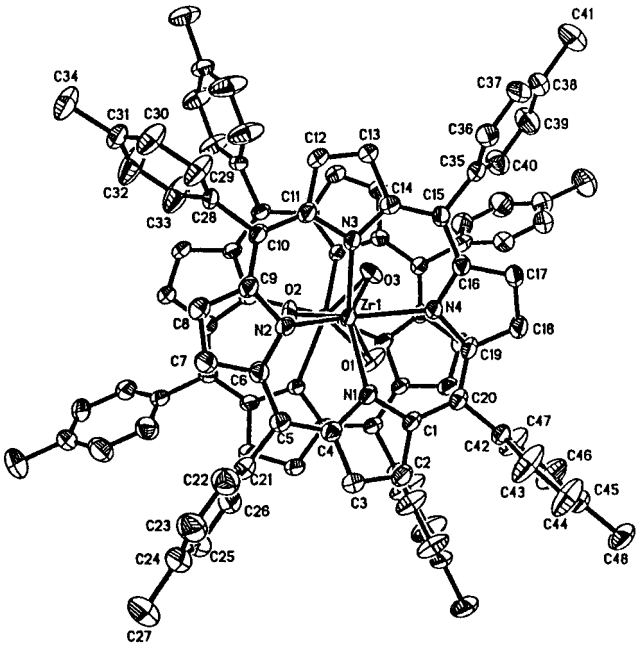

Figure 5. Top view of complex **5**, $[(TTP)Zr]_2(\mu\text{-}O)(\mu\text{-}OH)_2$. Thermal ellipsoids are drawn at the 50% probability level.

Scheme 1

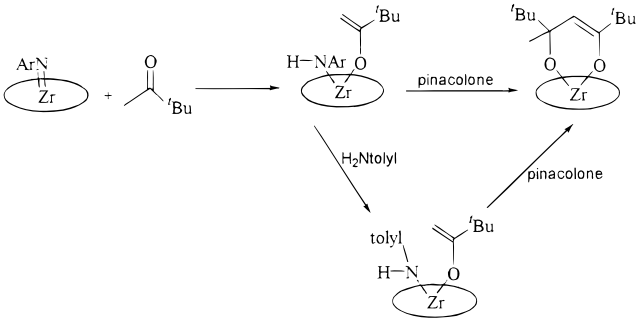

Scheme 2

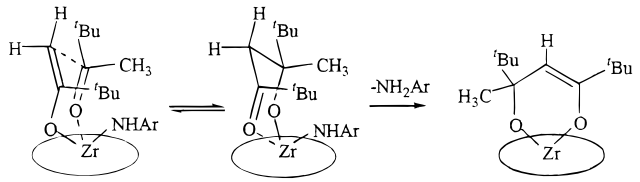

producing the hydroxo/enolato derivative.[16g] An amido/O-bound enolato species, **2a**, was found upon treatment of the imido complex **1** with 1 equiv of pinacolone. This enolate complex, **2a**, was inert in the presence of PhC≡CH, acetophenone, (TMS)Cl, or MeI at 80 °C in C_6D_6. The zirconium coordination sphere in **2a** appears to be sterically congested, as indicated by two observations. First, the ortho isopropyl groups of the NAr^{iPr} moiety are diastereotopic as a result of hindered rotation around the $N-C_{ipso}$ bond. Second, the bulky H_2NAr^{iPr} group is readily ejected on treatment with H_2N-tolyl to form (TTP)Zr(NH-tolyl)-[OC(=CH_2)(^{t}Bu)], **2b**. As expected, the reduced steric congestion of the tolyl amido/enolate species, **2b**, facilitates the formation of complex **2** in a substantially shorter time period (Scheme 1). The formation of complex **2** presumably involves a variation of the generally accepted aldol reaction mechanism (Scheme 2).[21] The reaction of transition metal enolate complexes with aldehydes or ketones generally results in the formation of η^1- or η^2-bound β-hydroxy ketone complexes.[22] However, as shown in Scheme 2, deprotonation of the η^2-hydroxy ketone complex by the strong base $NHAr^-$ results in the formation of a unique chelated enediolate product.[23]

Intractable mixtures were obtained from the addition of acetone to **1** or **2a**. However, the reaction between (TTP)Zr-($NHAr^{iPr}$)[OC(=CH_2)(^{t}Bu)], **2a**, and 2-octanone resulted in a new enediolate complex, (TTP)Zr[OC(^{t}Bu)CHC(hexyl)(Me)O]. Thus, this synthetic methodology may be extended to other ketones.

Bridging Oxo Complexes. An atom transfer route for the preparation of terminal oxo species of titanium porphyrin complexes was extended to Zr for the production of complex **4**.[24] Thus, the metathesis reaction between (TTP)Zr=NAr^{iPr} and nitrosobenzene cleanly produced the μ-oxo dimer **4**. The postulated transient monomeric oxo species (TTP)Zr=O could not be trapped in the presence of excess THF or pyridine. Compound **4** is unreactive toward ^{t}BuNCO, ketones, amines, and alcohols, including phenol. This lack of reactivity appears to be based, in part, on steric factors, since compound **4** is quickly hydrolyzed to compound **5**. Further reactivity of complex **5** was not observed in the presence of phenol, *tert*-butylamine, aniline, or $ZnEt_2$. A comparison of the structurally characterized oxygen-bridged complexes $[(TPP)Hf]_2(\mu\text{-}OH)_2(\mu\text{-}O)$,[15e] $[(TPP)Zr]_2(\mu\text{-}OH)_2(\mu\text{-}O)$,[15b] and $\{[(OEP)Zr]_2(\mu\text{-}OH)_3\}(7,8\text{-}C_2B_9H_{12})$[15b] shows near-eclipsing of an M−O bond with an M−N bond and the presence of eclipsed porphyrin rings. This has been attributed to pπ−dπ orbital interaction between the oxygen and the metal. Complex **5** does not possess eclipsed porphyrin rings. As the intramolecular steric properties of tetraphenylporphyrin are expected to be equivalent to those of tetratolylporphyrin, dπ−pπ interactions between the Zr and O atoms in complexes **4** and **5** are not readily apparent.[25]

It is interesting to note the structure of the only other known six-coordinate zirconium metalloporphyrin complex containing two O-bound ligands, (OEP)Zr(O^tBu)$_2$.[14b] First, the O−Zr−O angle of 90.08(9)° is rather large for this class of molecules.[26] Second, the zirconium out-of-plane distance of 1.06 Å is the largest value reported for six-coordinate zirconium metalloporphyrin complexes. Although these features were attributed primarily to the steric bulk of the O^tBu ligands, Zr−O π-bonding would most likely be enhanced by such an arrangement.[27] Zirconium lies further toward the porphyrin plane and contains an O1−Zr1−O2 angle of 78.56(8)° in complex **4**. The presence of dπ−pπ interactions is expected in complex **4**, albeit somewhat diminished, as evident in the metrical parameters described above.

Conclusion

New examples of the novel reactivity possessed by zirconium and hafnium imido metalloporphyrin complexes have been demonstrated. These complexes mediate the stepwise coupling

(21) Yamago, S.; Machii, D.; Nakamura, E. *J. Org. Chem.* **1991**, *56*, 2098.

(22) (a) Veya, P.; Cozzi, P. G.; Floriani, C.; Rotzinger, F. P.; Chiesi-Villa, A.; Rizzoli, C. *Organometallics* **1995**, *14*, 4101. (b) Veya, P.; Floriani, C.; Chiesi-Villa, A.; Rizzoli, C. *Organometallics* **1994**, *13*, 208.

(23) Aldol condensation reactions utilizing zirconium enolates have been well studied: Cozzi, P. G.; Veya, P.; Floriani, C.; Rotzinger, F. P.; Chiesi-Villa, A.; Rizzoli, C. *Organometallics* **1995**, *14*, 4092 and references therein.

(24) Thorman, J. L.; Woo, L. K. *Inorg. Chem.* **2000**, *39*, 1301.

(25) Bottomley, F.; Sutin, L. *Adv. Organomet. Chem.* **1988**, *28*, 339.

(26) Brand, H.; Arnold, J. *Coord. Chem. Rev.* **1995**, *140*, 137.

(27) Tatsumi, K.; Hoffmann, R. *J. Am. Chem. Soc.* **1981**, *103*, 3328.

of pinacolone in the formation of an enediolate compound. Mixed-ketone condensation products are also possible. Moreover, we have developed direct synthetic routes to zirconium metalloporphyrin complexes containing bridging oxygen ligands. (TTP)Zr═NAr^{iPr} undergoes metathesis with nitrosobenzene to produce the μ-oxo-bridged dimer, [(TTP)ZrO]$_2$, **4**. The bis(μ-hydroxo)(μ-oxo) dimer [(TTP)Zr]$_2$(μ-OH)$_2$(μ-O), **5**, is a hydrolysis product of complex **4**. Also of interest is the unique structural characteristic of staggered porphyrin rings found for complexes **4** and **5**. This is in marked contrast to the eclipsed conformers known for other Zr and Hf analogues.

Acknowledgment. We are grateful for financial support from the Camille and Henry Dreyfus Foundation.

Supporting Information Available: X-ray crystallographic files in CIF format, for **2**, **4**, and **5**. This material is available free of charge via the Internet at http://pubs.acs.org.

IC9910007